A Directional, Low-Profile Zero-Phase-Shift-Line (ZPSL) Loop Antenna for UHF Near-Field RFID Applications

YunjiaZeng[(1)], Xianming Qing[(1)], Zhi Ning Chen[(2)]

[(1)] Institute for Infocomm Research, Singapore

[(2)] National University of Singapore, Singapore

Abstract- A low-profile zero-phase-shift-line (ZPSL) loop antenna is proposed to achieve a directional magnetic near-field distribution for applications in ultra-high frequency (UHF) near-field radio-frequency identification (RFID). The proposed antenna consists of three coaxially-stacked components, including a driven ZPSL loop, a parasitic ZPSL loop, and a metallic plate reflector. Conventional directional antennas that involve metallic plate reflectors require an optimal separation of one-quarter of a wavelength at the operating frequency between the antenna and the plate. Decreasing the separation would result in poor impedance matching as well as a reduction in gain for far-field antennas. To realize a low-profile directional far-field antenna, a novel approach was recently proposed by adding a parasitic strip between a dipole antenna and a metallic plate reflector, such that the phase of the reflected wave can be properly controlled. In this manner, the separation between the antenna and the reflector is reduced to 0.05 of the operating wavelength, while keeping the reflected and the directly radiated fields in phase in the desired direction.

In this paper, such an approach is extended to the design of near-field antenna. Because of the geometry of the bi-directional ZSPL loop, the parasitic element is chosen as an aperiodic ZPSL loop that has the same geometry as the driven element to ensure a strong coupling between the two loops. In the design of near-field antennas, the current distributions of the antennas are the decisive factors affecting the near-field distributions. Therefore, the proposed antenna is designed based on the current distributions instead of the phase information as in the case of far-field antennas. The proposed antenna is fabricated and measured, and it proves to be an effective reader antenna for UHF near-field RFID applications.

1. INTRODUCTION

A ZPSL loop antenna consisting of single-line structures produces a bi-directional magnetic field distribution in the near-field zone of the antenna [1]. However, a directional field distribution is more desirable for certain applications such as an RFID smart shelf [2]. The conventional approach to realizing a directional field distribution involves applying a large metal plate as a reflector of an antenna, in which the reflector cannot be placed very close to the antenna to avoid a significant reduction of the magnetic field intensity in the desired region. This is because the eddy current induced on the reflector is in the opposite direction to that on the antenna, and decreasing the separation between the antenna and the reflector would result in field cancellation as well as poor impedance matching. In [3], the distance between a near-field ZPSL loop antenna and a metal plate reflector was set as $\lambda_0/8$ (with λ_0 being the free-space wavelength at the operating frequency), which would significantly increase the thickness of the antenna, in particular, at lower frequency bands. One effective approach is to use an AMC reflector to replace the metal plate, such that the distance between the antenna and the reflector can be reduced and the magnetic field intensity can be further enhanced [4]. Nevertheless, it is nontrivial to design an AMC reflector and to integrate the reflector with a ZPSL loop antenna. Moreover, the fabrication cost increases when complex structures are employed in an AMC reflector.

Conventional directional far-field antenna designs that involve metal plate reflectors require a $\lambda_0/4$ separation between the radiator and the reflector, which increases the thickness of the antenna significantly. A reduced separation is able to make the antenna low profile while leading to poor impedance matching and degradation in radiation efficiency, due to the out-of-phase current induced on the reflector. A simplified approach of designing a directional low-profile far-field antenna has recently been proposed, wherein a parasitic strip was added in between a dipole antenna and a metallic ground plane [5]. The parasitic strip introduces an additional phase shift to compensate for the effects of the out-of-phase current on the ground.

With this, the dipole antenna can be positioned very close to the metallic ground plane and the separation between the antenna and the ground can be significantly reduced to $\lambda_0/20$.

In this paper, the approach of applying a parasitic strip in between a dipole and a ground is extended to the case of ZSPL loops. A low-profile ZPSL loop antenna is proposed to achieve a directional magnetic field distribution for UHF near-field RFID applications. The antenna has a low profile of 0.046 of the operating wavelength at 915 MHz, achieving a desired directional magnetic field distribution over a circular interrogation zone with a perimeter of 1.5 times the operating wavelength. The proposed design is tested as a UHF near-field RFID reader antenna, and achieves much enhanced performance than a single ZPSL loop.

2. ANTENNA DESIGN

The proposed antenna design is shown in Figure 1. The antenna consists of a driven ZPSL loop, a parasitic ZPSL loop, and a metallic ground plane. The driven and parasitic loops are printed on two pieces of single-layer FR4 substrates (ε_r = 4.3 and tan δ = 0.025, thickness of 32 mils, or 0.8128 mm), respectively. Figure 1(a) exhibits the driven element, which is an aperiodic ZPSL loop antenna with nonuniformly arranged unit cells that are shown in Figure 1(b). The length of the unit cell, L, varies from 52 to 80 mm (L_1 = 80 mm, L_2 = 64 mm, and L_3 = 52 mm). The radius R of the driven ZPSL loop is 80 mm. As suggested in [6], the aperiodic ZPSL loop antenna is able to generate a more uniform current flowing along the loop, which results in a more uniform magnetic field distribution with an enhanced magnetic field intensity. In Figure 1(c), the parasitic ZPSL loop is a closed aperiodic ZPSL loop with the same configuration as the driven one. Figure 1(d) presents the cross-section view of the design. The two ZPSL loop elements and the ground plane are coaxially stacked in the z-direction, with the driven element placed 5 mm above the parasitic element, which is positioned 10 mm above the ground.

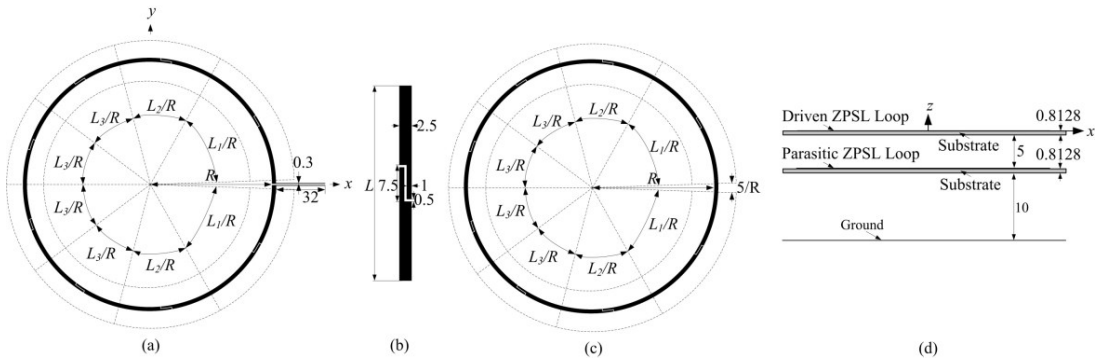

Figure1: Configurations of the proposed antenna design: (a) driven ZPSL loop; (b) ZPSL unit cell structure; (c) parasitic ZPSL loop; and (d) cross-section view of the antenna. (unit: mm).

Unlike in [5], the phase information in the far-field approximation cannot be applied to design the near-field antenna. The proposed antenna is designed based on the current distributions on the elements of the antenna, among which the effect of the parasitic ZPSL loop is significant. Considering a single loop with an in-phase current flow, the current induced on a nearby ground plane is in the opposite direction to that of the single loop. Since the out-of-phase currents are positioned closely, they cancel each other out and lead to reduced magnetic field intensity and non-uniform magnetic field distribution. In order to compensate for the effects of such a current cancellation, it is intuitive to assume that the parasitic ZPSL loop needs to carry a current of the same phase as that of the single loop. In Figure 2, the simulated current distribution of each part of the proposed antenna is shown. It can be observed that the driven and parasitic elements carry almost the same current. Figure 2(c) presents the current distribution on the ground plane, and the plotted region has the same size as the ZPSL loops. Several closed-loop currents are observed on the ground plane, with each of the currents flowing in the opposite direction to those on the ZPSL loops.

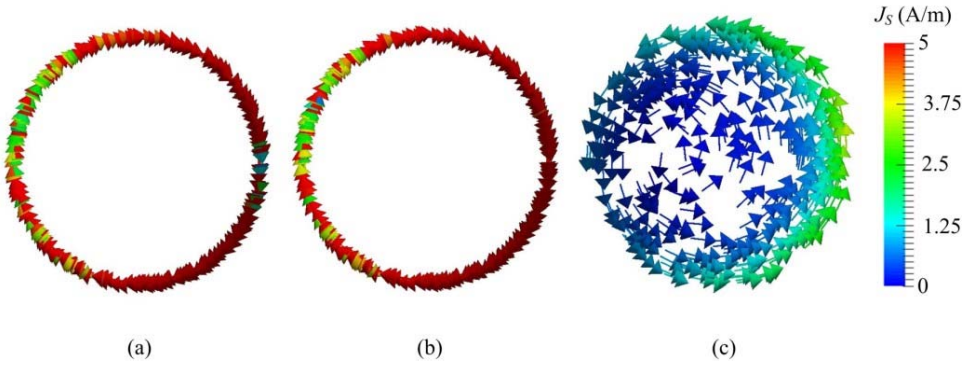

Figure 2: Simulated current distributions of the proposed antenna: (a) driven element; (b) parasitic element; and (c) ground plane.

In order to verify the assumption on current distributions, the simulated magnetic field distribution along the *z*-axis of the proposed antenna design is examined in Figure 3. Compared with the distribution of the single driven ZPSL loop, the proposed antenna exhibits a directional magnetic field distribution, with the magnetic field in the negative *z* direction decreased by over 10 dB. Another structure considered is the single driven ZPSL loop backed with a ground plane, which is constructed similar to the proposed antenna but with the parasitic ZPSL loop removed. It can be observed that the proposed design exhibits an enhanced magnetic field intensity compared to the case of a single ZPSL loop with a ground plane. When *z* increases above 20 mm, the magnetic field intensity of the proposed design becomes greater than that of the single ZPSL loop. The observation validates the assumption about the current distribution of the parasitic ZPSL loop.

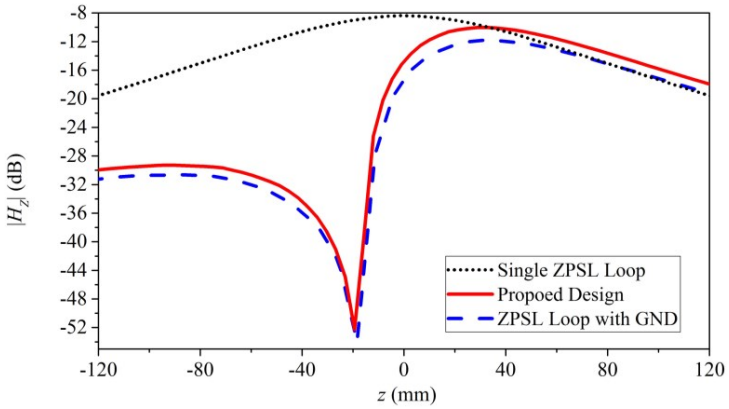

Figure 3: Simulated magnetic field distributions of the proposed antenna, the single ZPSL loop, and the single ZPSL loop with ground.

Figure 4 presents the impedance characteristic of the proposed antenna. Three antennas are examined, including the proposed antenna, the single driven ZPSL loop, and the single ZPSL loop backed with a ground plane. In Figure 4(b), it is interesting to note that the proposed antenna shows a much higher input resistance than that of the single ZPSL loop, while the case without a parasitic ZPSL loop exhibits the lowest input resistance. It suggests that the in-phase current that flows along the parasitic ZPSL loop in the proposed design helps alleviate the current cancellation effects caused by the ground plane.

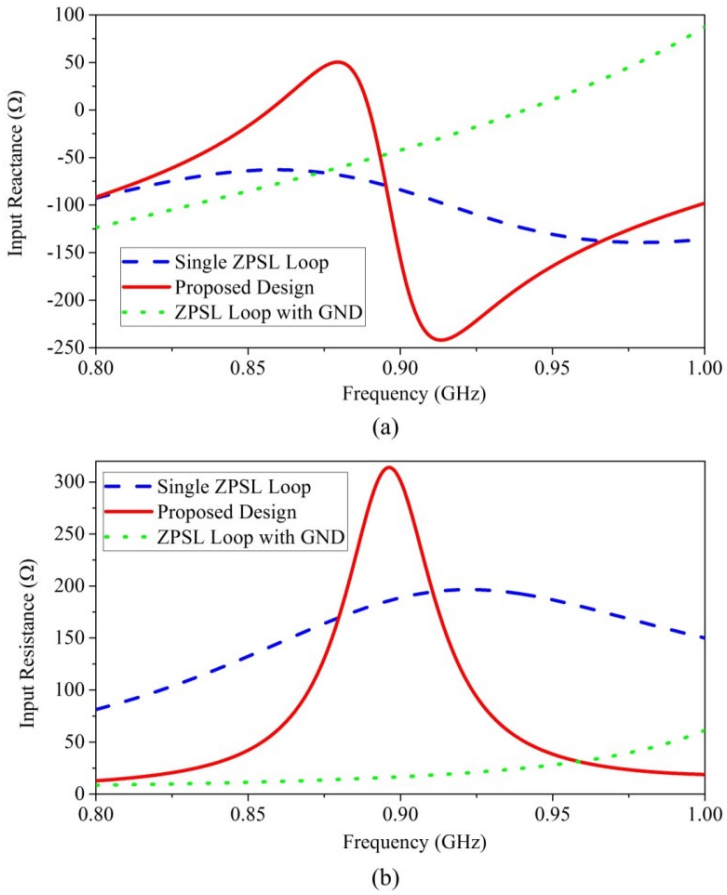

Figure 4: Simulated input impedance of the proposed antenna: (a) reactance; and (b) resistance.

3. ANTENNA IMPLEMENTATION AND MEASUREMENT

Based on the parameters given in Section 2, the proposed antenna is fabricated and measured. Figure 5 compares the simulated and measured reflection coefficients of the antenna. The proposed antenna achieves -10 dB reflection coefficient in the frequency band ranging from 902 to 931MHz.

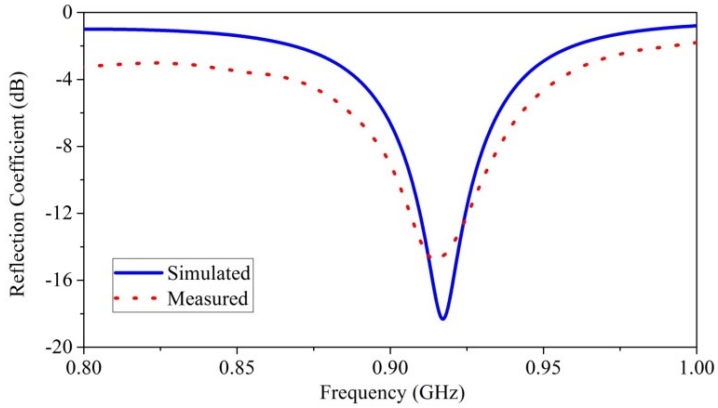

Figure 5: Simulated and measured reflection coefficients of the proposed antenna.

Figure 6(a) shows the measurement set-up of magnetic field distribution of the antenna. The self-built near-field scanning system includes a three-dimensional scanner, a vector network analyzer, and a near-field probe such as the Langer EMV-Technik RF-R 3-2 probe. The magnetic field distributions in three planes that are parallel to and above the measured antenna are obtained by scanning the probe with an interval of 5 mm. Figure 6(b) presents the set-up of the UHF RFID tag-reading test, wherein the antenna serves as the reader antenna. An Impinj Speedway UHF reader with an output power of 30 dBm is used to read 50 pieces of SAG round tags.

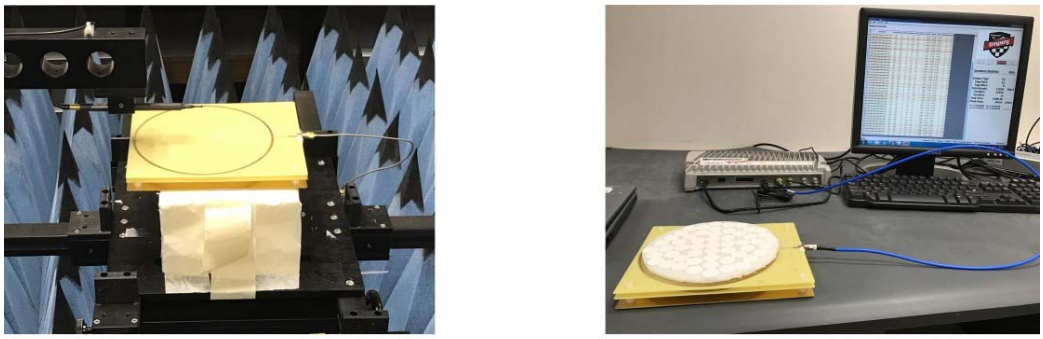

(a) (b)

Figure 6: (a) Magnetic field distribution measurement set-up and (b) UHF RFID tag-reading rate test.

Figure 7 displays the magnetic field distributions ($|H_z|$) at 915 MHz of the antennas measured under the same conditions. The magnetic field distributions are measured in the planes of z = 40, 80, and 120 mm, with z = 0 mm aligning with the top surfaces of the antennas. In all three planes, the proposed antenna exhibits an enhanced magnetic field distribution compared with that of the single ZPSL loop. Figure 8 shows a good agreement between the simulated and measured magnetic field distributions of the proposed antenna. The simulated results are normalized to the maximum values of the corresponding measured two-dimensional distributions.

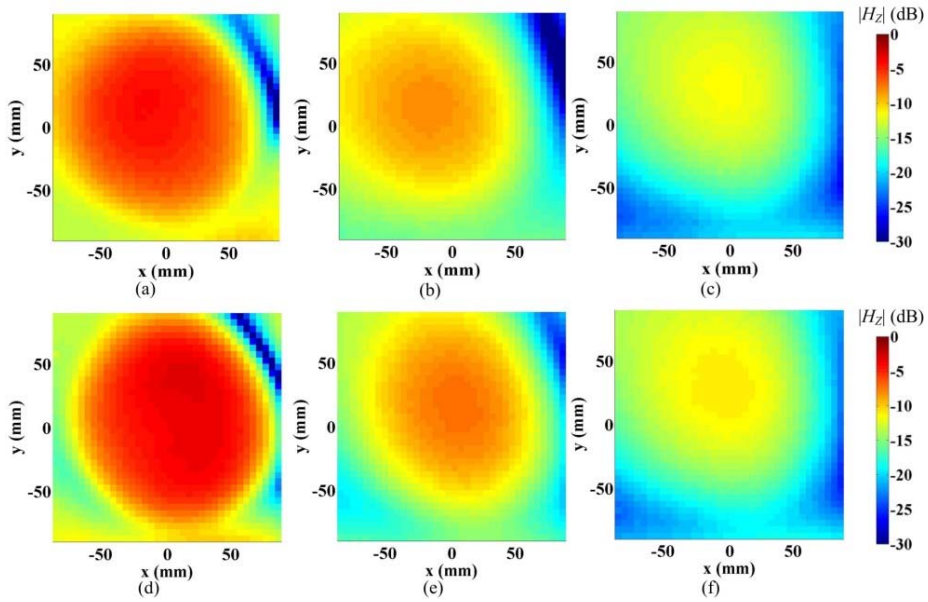

Figure 7: Measured magnetic field distributions at 915 MHz. Single ZPSL loop: (a) z= 40 mm; (b) z= 80 mm; and (c) z = 120 mm. Proposed antenna: (d) z= 40 mm; (e) z= 80 mm; and (f) z = 120 mm.

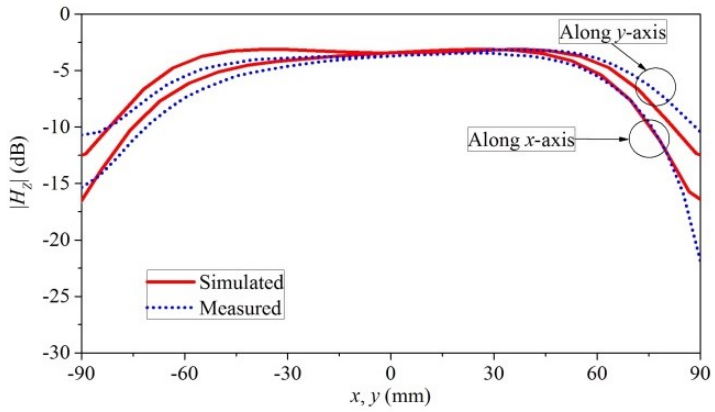

Figure 8: Simulated and measured magnetic field distributions of the proposed antenna along the x- and y-axes in the plane of z = 40 mm at f = 915 MHz.

Figure 9 compares the tag-reading rates of the proposed antenna and the single ZPSL loop, again measured under the same conditions with the same input power of 30 dBm. The configuration of a SAG tag is shown in the inset of Figure 9. The proposed antenna achieves 100% tag detection up to a reading distance of 110 mm. The proposed antenna proves to be an effective reader antenna with much enhanced performance for UHF near-field RFID applications.

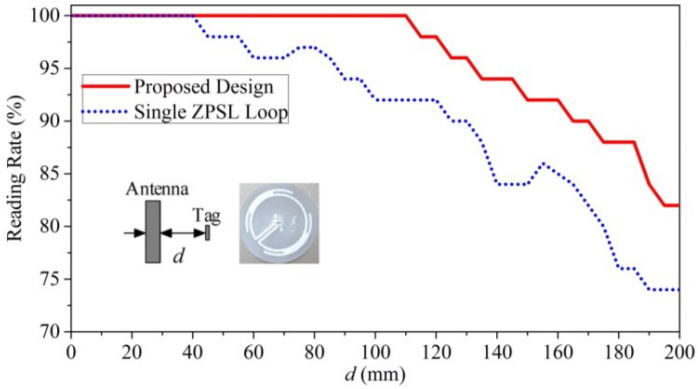

Figure 9: Measured tag-reading rate against reading range.

4. CONCLUSION

In this paper, a directional, low-profile ZPSL loop antenna has been proposed for UHF near-field RFID applications. The current distributions on the proposed antenna have been analyzed to achieve the desired magnetic near-field distribution. The parasitic ZPSL loop element of the proposed design realizes an in-phase current distribution as the driven element, and thus helps reduce the current cancellation caused by the out-of-phase current on the ground plane. Compared with a single ZPSL loop, the proposed ZPSL antenna has demonstrated a significantly improved performance as a UHF near-field RFID reader antenna.

REFERENCES

1. Y. Zeng, Z. N. Chen, X. Qing, and J. M. Jin, "Modeling and characterization of zero-phase-shift line (ZPSL) and optimization of electrically large ZPSL loop antennas for near-field systems," *IEEE Trans. Antennas Progag*., vol. 64, no. 11, pp. 4587–4593, 2016.

2. Y. Yao, C. C, Y. J, and C. X, “A meander line UHF RFID reader antenna for near-field applications,” *IEEE Trans. Antennas Progag*.,vol. 65, no. 1, pp. 82–91, 2017.
3. X. Qing, C. K. Goh, and Z. N. Chen, “A broadband UHF near-field RFID antenna,” *IEEE Trans. Antennas Progag*., vol. 58, no. 12, pp.3829–3838, 2010.
4. Y. Zeng, Z. N. Chen, X. Qing, and J. M. Jin, “An artificial magnetic conductor backed electrically large zero-phase-shift line grid-loop nearfield antenna,” *IEEE Trans. Antennas Progag*., vol. 65, no. 4, pp. 1599–1606, 2017.
5. Z. N. Chen, Y. Juan, X. Qing, and W. Che, “Enhanced radiation from a horizontal dipole closely placed above a PEC ground plane using a parasitic strip,” *IEEE Trans. Antennas Progag*., vol. 64, no. 11, pp.4868–4871, 2016.
6. Y. Zeng, Z. N. Chen, X. Qing, and J. M. Jin, “Design of a near-field nonperiodic zero-phase-shift-line (ZPSL) loop antenna with a full dispersion characterization,” *IEEE Trans. Antennas Progag*., vol. 65, no. 5,pp. 2666–2670, 2017.